PID, 2-DOF PID and Mixed Sensitivity Loop-Shaping Based Robust Voltage Control of Quadratic Buck DC-DC Converter

Fateh OUNIS, Noureddine GOLEA

Electrical Engineering Department, Sciences and Applied Sciences Faculty, Larbi Ben M'hidi University, 04000 Oum El Bouaghi, Algeria

ounisfateh_01@yahoo.fr, nour_golea@yahoo.fr

DOI: 10.15598/aeee.v14i5.1821

Abstract. *DC-DC Quadratic Buck Converter (QBC) is largely used in applications where the high step-down conversion ratio is required. In the practical implementation, QBC is subject to uncertainties, disturbance, and sensor noise. To address the QBC control problems, a two-degree of freedom PID (2-DOF PID) is designed in the robust control framework. Further, for comparison purpose, a one-degree of freedom PID (1-DOF PID) and mixed sensitivity loop-shaping (MS-LS) controller are also proposed. Considering QBC parasitic components, the QBC small-signal transfer function is derived based on a practical approach. Sensitivity functions are used to specify the desired design requirements, and non-smooth optimization is used to tune both PID's parameters. The three control structures are implemented and tested in the Matlab/Simulink environment. As attested by simulation results, the 2-DOF PID exhibits a better regulation accuracy with enhanced robust stability and robust performance for a wide range of supply voltage/load variation and sensor noise effect.*

Keywords

DC-DC converters, mixed sensitivity, loop-shaping, PID control, quadratic buck converter, robust control.

1. Introduction

DC-DC converters are key elements in power energy modulation and conversion. Basic DC-DC converters, such as buck, boost and buck-boost, are widely used in various fields of technology [1]. Recently, new applications, such as LED lamps, microprocessors, portable devices and GPS, require very low dc voltages and they operate at very high currents. Such applications require converters with low ripples in the voltage and current and high efficiency in order to achieve precise output voltage regulation against parameter, line and load disturbances. Basic step-down converters are not suitable for high step-down voltage conversion since operating at a small duty ratio affects the converter dynamic performance and cause asymmetry in the on and off times of the switches. Moreover, very small duty ratio limits the converters switching frequency and increases peak switch current that leads to more switching losses, severe reverse-recovery problems and converter's efficiency degradation [2]. Some cascade interconnected power converters structures were developed to face this problem [3]. However, a notable disadvantage of cascaded converters is that the overall efficiency is reduced by losses in switching devices. To improve overall efficiency, Quadratic Buck Converters (QBC) were developed in [4], [5], [6] and [7]]. QBC is designed based on cascade connection of two buck converters and has only one active switching device. The DC conversion ratio is the product of the conversion ratios of the two single buck converters. QBC operates at higher switching frequencies with wide load range and achieves an improved step-down conversion ratio. The efficiency is also enhanced since only one active switch is used [8] and [9].

As QBC exhibits complex nonlinear dynamics subject to parameters uncertainties and input/load variations, control loops must be introduced to guarantee stability and operating performance. Several QBC control techniques such as linear state feedback, feedback linearization, sliding mode control and passivity based control, were presented in [10]. In [11], QBC nonlinear control scheme is proposed. QBC with LC input filter and damping control is developed in [12].

Robust QBC control based on identified Hammerstein model is proposed in [13]. Average current-mode control for the QBC is proposed in [14], where the outer voltage control loop bandwidth is limited by inner current control loop bandwidth. In [15], robust control for QBC is designed based on Kharitonov's theorem and D-stability concept. To ensure robust output regulation, robust state feedback stabilizer with saturated internal model, is proposed in [16]. In [17], inner current loop PI parameters are selected from QBC large-signal model, and outer voltage loop is controlled using a conventional PI regulator. To ensure robustness in the presence of disturbances and uncertainties, H_∞ based control is investigated in [18].

In this paper, 2-DOF PID is developed to solve the QBC robust control problem. For the comparison, a 1-DOF PID and MS-LS control are also proposed. Taking the parasitic components into account, the QBC small signal transfer function from output voltage to control signal is derived. Robust performance requirements are defined using the same weighting functions for both PID and by another set of weighting functions for MS-LS control. Contrary to MS-LS control and 1-DOF PID, the 2-DOF PID provides a wide range of the crossover frequency to specify response time-performance compromise. The non-smooth approach presented in [19] is used to tune both PID's parameters. Based on the model reduction methods, MS-LS controller is reduced from 8 to 5, and the reduced version is presented and used in simulations. Simulation results illustrate the 2-DOF PID in term of accuracy and stability robustness.

The remainder of this paper is organized as follows. Section 2. presents the QBC nominal transfer function computation. The MS-LS control is developed in Section 3. PID controller's design is provided in Section 4. The three controllers' robustness analysis is established in Section 5. Simulation results are shown in Section 6. Concluding remarks are given in Section 7.

2. QBC Nominal Model

As a first step for the control design, the QBC open loop small-signal control-to-output voltage transfer function should be established. The objective can be reached using analytical modeling and averaging techniques [20] and [21]. In this work, a practical approach is adopted. Based on QBC parameters and operating point given in App. A, a Simulink implementation of the open loop excitation is realized (Fig. 1). The PWM control signal duty cycle is adjusted to get the desired output voltage level. Taking into account the parasitic components, the QBC discrete-time transfer function $G(z) = B(z)/A(z)$ is assumed of 6^{th} order. Hence,

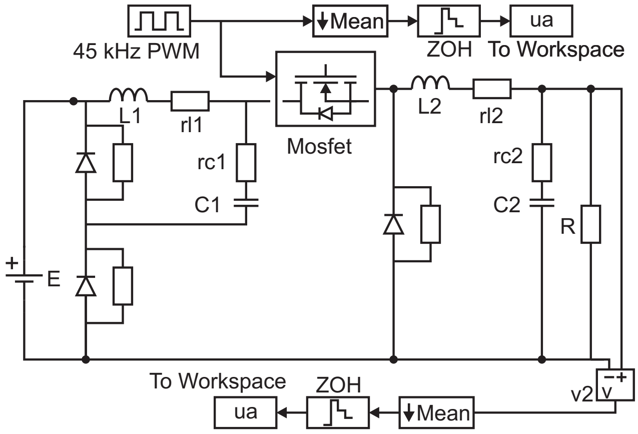

Fig. 1: QBC open loop excitation setup.

applying the Steiglitz-McBride recursive identification method [22] on converter averaged input/output signals for 5 iterations, yields the estimated transfer function:

$$\begin{aligned} B(z) &= 0.7108 - 1.6654z^{-1} + 1.9263z^{-2} \\ &\quad -1.6483z^{-3} + 1.2154z^{-4} - 0.5151z^{-5}, \\ A(z) &= 1 - 4.829z^{-1} + 10.1746z^{-2} - 11.9259z^{-3} \\ &\quad +8.1753z^{-4} - 3.1028z^{-5} + 0.5094z^{-6}. \end{aligned} \tag{1}$$

Further, using the numerical algorithm proposed in [23], the equivalent continuous-time transfer function $G(s) = N(s)/D(s)$ is given by:

$$\begin{aligned} N(s) &= 544300s^5 + 1.618 \cdot 10^{11}s^4 + \\ &\quad +2.184 \cdot 10^{18}s^3 + 1.524 \cdot 10^{23}s^2 + \\ &\quad +7.774 \cdot 10^{29}s + 3.487 \cdot 10^{34}, \\ D(s) &= s^6 + 674400s^5 + 7.804 \cdot 10^{11}s^4 + \\ &\quad +3.354 \cdot 10^{17}s^3 + 1.502 \cdot 10^{23}s^2 + \\ &\quad +2.677 \cdot 10^{28}s + 2.342 \cdot 10^{33}. \end{aligned} \tag{2}$$

The $G(s)$ Bode plot is shown in Fig. 2. It is clear that QBC has two second-order filters with high quality-factor Q, which depends on the selected circuit values. All poles and zeros are located on the right half of the s-plane as shown the Fig. 3. The right half plane zeros are responsible for the excessive phase lag in the ideal case. The Equivalent Series Resistances (ESR) provide some damping into the system, which is beneficent as it will ease feedback control design.

3. MS-LS Control Design

A diagram of the control design is shown in Fig. 4, where G is the quadratic buck converter transfer function. W_1, W_2 and W_3 are the performance, control and noise weighting functions, respectively. Further, w denote input signals, z output vector that includes

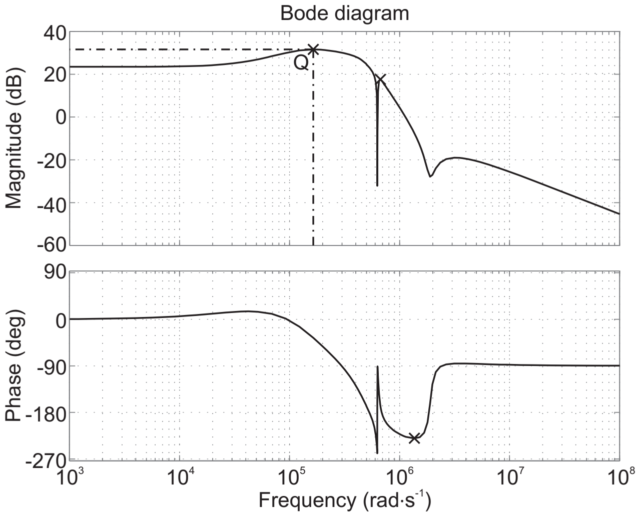

Fig. 2: Frequency open loop QBC response.

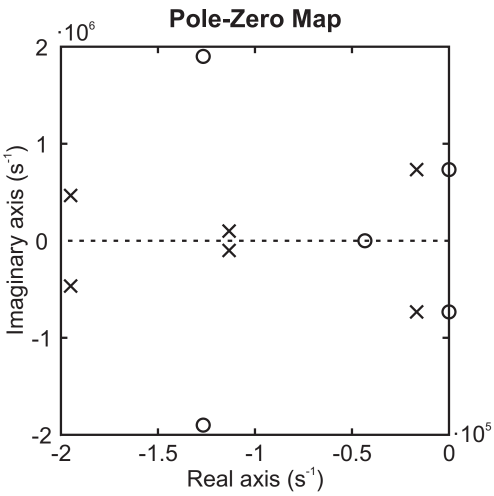

Fig. 3: Transfer function pole-zero map.

both performance and robustness measures, v is the vector of measurements available to the controller K and u the control signal. In the context, the necessary definitions are given by:

$$S(s) = \big(I + G(s)K(s)\big)^{-1}, \tag{3}$$

$$T(s) = G(s)K(s)\big(I + G(s)K(s)\big)^{-1}, \tag{4}$$

where $S(s)$ is the sensitivity function and $T(s)$ is the complementary sensitivity function. The generalized closed loop transfer function is given by:

$$T_{zw} = \begin{bmatrix} W_1 S \\ W_2 RS \\ W_3 T \end{bmatrix}, \tag{5}$$

where $R(s) = K(s)\big(I + G(s)K(s)\big)^{-1}$. In this mixed problem, the control objective is to design a stable controller that minimizes the norm of the generalized

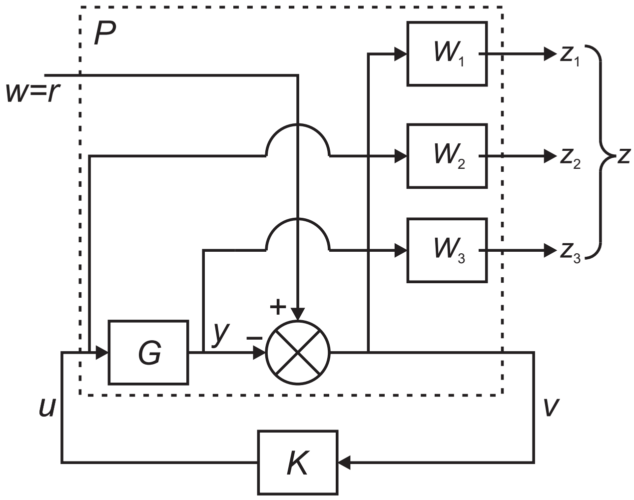

Fig. 4: MS-LS control design.

transfer function T_{zw} such that:

$$||T_{zw}||_\infty < 1. \tag{6}$$

3.1. Weighting Functions Selection

The closed loop performance of the system is largely dependent on the shape of the weighting function. The weight function W_1 specifies the control performance and W_1 is selected according to methodology suggested by Zhou [24],

$$W_1 = \frac{s/M_s + w_s}{s + w_s e_s}, \tag{7}$$

where e_s is the maximum allowed steady-state offset fixed to $e_s = 0.001$, w_s is the desired bandwidth fixed to $6 \cdot 10^3$ rad·s^{-1} and M_s is the sensitivity peak (typically $M = 1.6$). Therefore,

$$W_1 = \frac{0.625(s + 9600)}{s + 6}. \tag{8}$$

In order to avoid impulsive input effect on the converter, W_2 is chosen as:

$$W_2(s) = 0.01. \tag{9}$$

W_3 is used to shape the complementary sensitivity function T, and thus it must be large at high frequencies. Hence W_3 is chosen as:

$$W_3 = \frac{s + w_b/M_b}{e_b s + w_b}. \tag{10}$$

To keep the system stable, the complementary sensitivity T must be small for high frequencies. Thus, the value 0.001 is selected for the parameter e_b. In order to limit the closed loop bandwidth, the parameter M_b is fixed as 1.6 and w_b is fixed to 10^4 rad·s^{-1}. Then:

$$W_3 = \frac{1000(s+6250)}{s+10^7}. \tag{11}$$

In order to adopt a unified solution procedure, the above matrix inequality Eq. (6) can be recast into a standard configuration as in Fig. 4. This can be obtained by using the Linear Fractional Transformation (LFT), and the generalized plant P is obtained by grouping signals into sets of external inputs, outputs, input to the controller and output from the controller, which yields:

$$\left[\frac{z}{v}\right] = \underbrace{\left[\begin{array}{c|c} W_1 & -W_1 G \\ 0 & W_2 G \\ 0 & W_3 G \\ \hline \mathrm{I} & -G \end{array}\right]}_{P} \left[\frac{r}{u}\right], \tag{12}$$

where $r = w$ is the reference voltage, $z = \begin{bmatrix} z_1 & z_2 & z_3 \end{bmatrix}^T$ is the output signals vector, is the control signal and is the controlled QBC output voltage. W_1, W_2 and W_3 are the weighting functions described by Eq. (8), Eq. (9) and Eq. (11), respectively.

Based on the above configuration, the generalized plant can be built up, and consequently the controller can be calculated using Matlab robust control toolbox. Hence, the obtained 8$^{\text{th}}$ order controller is:

$$K(s) = \frac{N_K(s)}{D_K(s)}, \tag{13}$$

with

$$\begin{aligned} N_K(s) &= 5.504 \cdot 10^6 s^7 + 5.875 \cdot 10^{13} s^6 + 4.141 \cdot 10^{19} s^5 \\ &+ 4.48 \cdot 10^{25} s^4 + 1.929 \cdot 10^{31} s^3 + 8.414 \cdot 10^{36} s^2 \\ &+ 1.486 \cdot 10^{42} s + 1.289 \cdot 10^{47}, \end{aligned}$$

and

$$\begin{aligned} D_K(s) &= s^8 + 5.444 \cdot 10^9 s^7 + 5.525 \cdot 10^{15} s^6 \\ &+ 2.3 \cdot 10^{22} s^5 + 1.718 \cdot 10^{28} s^4 + 8.868 \cdot 10^{33} s^3 \\ &+ 5.922 \cdot 10^{39} s^2 + 2.5 \cdot 10^{44} s + 1.5 \cdot 10^{45}. \end{aligned}$$

The obtained controller Eq. (13) has high order, and can be further, reduced by examining $K(s)$ Hankel singular values σ_i. Hankel singular values based model reduction routines are grouped by the types of error bound. In Balanced Truncation (BT) and related methods, an error bound is a measure of how close the reduced order controller $K_r(s)$ is to the original system and is computed based on the infinity norm of the additive error,

$$||K(s) - K_r(s)||_\infty = \sum_{r+1}^{n} (\sigma_i), \tag{14}$$

with

$$K_r = \frac{N_{K_r}(s)}{D_{K_r}(s)}. \tag{15}$$

The basic idea of BT relies on balancing the two controllers' controllability Gramian and operability Gramian [25]. The Hankel singular values plotted in Fig. 5 are used to decide which states of the controller can be safely discarded. To achieve at least 1 % relative accuracy, the lowest-order controller $K_r(s)$ should be compatible with the desired level of accuracy chosen to be 5.

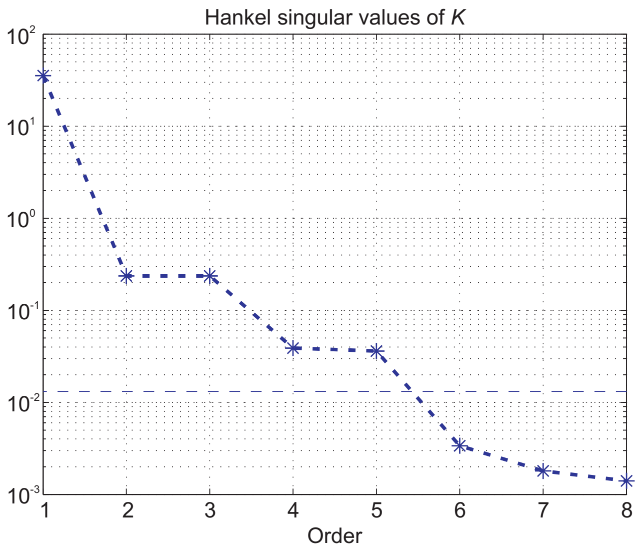

Fig. 5: Hankel singular values of $K(s)$.

The function "reduce" is the gateway to all model reduction routines available in the toolbox MATLAB. We use the default, square-root balance truncation ('balancmr') option of "reduce" as the first step. This method uses an "additive" error bound for the above described reduction method, meaning that it tries to keep the absolute approximation error uniformly small for all frequencies.

The error bound for additive-error algorithms is defined as:

$$||K(s) - K_r(s)||_\infty = 2(\sigma_6 + \sigma_7 + \sigma_8) = 0.0088, \tag{16}$$

which yields:

$$\begin{aligned} N_{K_r}(s) &= 1.045 \cdot 10^4 s^4 - 3.36 \cdot 10^9 s^3 + 5.937 \cdot 10^{15} s^2 \\ &- 1.393 \cdot 10^{21} s + 6.808 \cdot 10^{26}, \end{aligned}$$

$$\begin{aligned} D_{K_r}(s) &= s^5 + 2.848 \cdot 10^5 s^4 + 4.018 \cdot 10^{12} s^3 \\ &+ 1.128 \cdot 10^{17} s^2 + 1.43 \cdot 10^{24} s + 7.464 \cdot 10^{24}. \end{aligned}$$

According to condition Eq. (6), it is necessary that the magnitude response of S lies bellow the magnitude response of W_1^{-1} in the whole frequency range, and the magnitude response of T should lie bellow the response of W_3^{-1}. Figure 6 shows that these conditions are verified using the reduced controller.

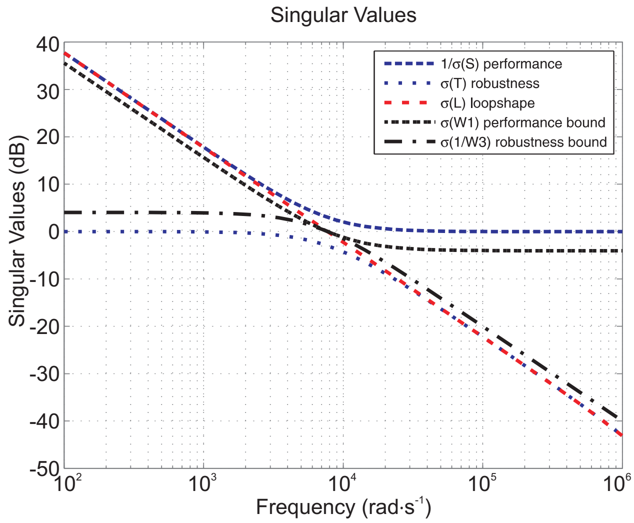

Fig. 6: MS-LS control design results.

4. 1-DOF PID and 2-DOF PID Controllers Design

In the following section, the control system structure of Fig. 7 is adopted, where $C(s)$ is the standard controller, $C_F(s)$ the input filter, and G is the converter transfer function.

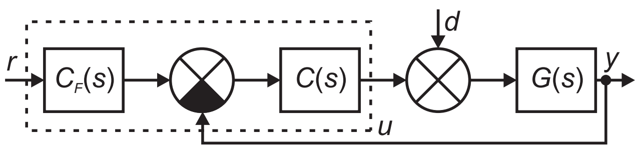

Fig. 7: 2-DOF PID structure.

The standard PID controller is used with the transfer function:

$$C(s) = K_P + \frac{K_I}{s} + \frac{K_D s}{T_f s + 1}, \tag{17}$$

with the proportional gain K_P, the integrator gain K_I, the derivative gain K_D, and the derivative filter time constant T_f.

4.1. 2-DOF PID Controller

The output signal of a 2-DOF regulator is defined as:

$$u(s) = K_P e_p + K_I e_I + K_D e_D, \tag{18}$$

where

$$\begin{cases} e_p = br(s) - y(s) \\ e_I(s) = \dfrac{1}{s}\big(r(s) - y(s)\big) \\ e_D(s) = \big(cr(s) - y(s)\big) \end{cases}, \tag{19}$$

where b, c are weighting parameters for proportional term and derivative term, respectively. The 2-DOF controller can be transformed into a 1-DOF controller, if b and c are selected to be equal to 1. To formulate the closed loop transfer function, the output of controller Eq. (19) is rewritten as:

$$u(s) = \big(C_F(s)r(s) - y(s)\big)C(s). \tag{20}$$

The closed loop control system output to the perturbation is given by:

$$y(s) = \frac{C_F(s)G(s)}{1 + C(s)G(s)} r(s) + \frac{G(s)}{1 + C(s)G(s)} d(s). \tag{21}$$

The system closed loop transfer function is defined as:

$$T_{yr}(s) = C_F(s)\frac{C(s)G(s)}{1 + C(s)G(s)}. \tag{22}$$

The parameters $\{K_P, T_I, T_D, b, c\}$ are obtained considering the targeted specifications.

4.2. Frequency Specifications

To ensure that the output voltage tracks the reference with a desired response time and tracking error, transfer function is used to specify the maximum frequency-domain tracking error:

$$e_{\max} = \frac{A_e s + \omega_c D_e}{s + \omega_c}, \tag{23}$$

where $\omega_c = 2/t_s$ (t_s is the settling time) is the tracking bandwidth, D_e is the maximum relative steady-state error and A_e is the peak relative error across all frequencies. For the QBC, we set $D_e = 0.001$, $A_e = 1$ and $\omega_c = 10^3$ rad·s^{-1}, since the open loop-gain should be high within the control bandwidth. To ensure good disturbance rejection, the minimum loop gain profile is chosen as:

$$W_s = \frac{0.03 w_c}{s}. \tag{24}$$

To ensure insensitivity to measurement noise, the open loop gain should be less than 1 outside the control bandwidth, so the maximum loop gain profile is chosen as:

$$W_T = \frac{0.3 w_c}{s}. \tag{25}$$

Using software provided by Matlab, the above requirements are converted into normalized scalars functions $f(x)$ and $g(x)$ such as:

$$g(x) = \left\| \frac{1}{e_{\max}} \big(T(s,x)\big) \right\|_{\infty}. \tag{26}$$

$$f(x) = \left\| \begin{matrix} W_s S_a \\ W_T^{-1} T_a \end{matrix} \right\|_\infty, \tag{27}$$

where $T(s,x) = \dfrac{L}{1+L}$ is the output complementary sensitivity function, $L(s,x)$ is the open-loop response being shaped, $T_a = D^{-1}TD$ is the scaled output complementary sensitivity function, $S_a = D^{-1}\left[(1+L(s,x))\right]^{-1}D$ is the scaled output sensitivity function, x is the vector of free (tunable) parameters K_P, K_I and K_D.

Then, determining the PID parameters is equivalent to solving the optimization problem:

$$\min_x \max\big(af(x), g(x)\big), \tag{28}$$

where $a > 0$ is a parameter weighting the subproblems importance in order to get the most optimal solution for the optimization problem. Nonsmooth optimization algorithms [26] and [27] are used to solve the QBC converter control problem. According to the required desirable performance, the ultimate PIDs parameters are achieved as follows:

1-DOF: $K_p = 0.00865$, $K_I = 230$, $K_D = -8.03 \cdot 10^{-5}$,
2-DOF: $K_p = 0.00824$, $K_I = 298$, $K_D = 1.68 \cdot 10^{-5}$, $b = 0.00015$, $c = 0.226$.

5. Robust Analysis

We can test the robustness properties of the three controllers by executing the proper μ tests for the QBC uncertain feedback system shown in Fig. 8, where the dashed box represents the QBC real transfer function G_{unc}. The transfer functions W_{del} and Δ_G parameterize the multiplicative uncertainty at the converter input. The transfer function W_{del} is assumed known, and the transfer function Δ_G is assumed to be stable and unknown, except for the norm condition $||\Delta_G||_\infty < 1$. The uncertainty weight W_{del} is described as:

$$W_{del}(s) = \frac{100s + 7.035 \cdot 10^7}{s + 7.035 \cdot 10^8}. \tag{29}$$

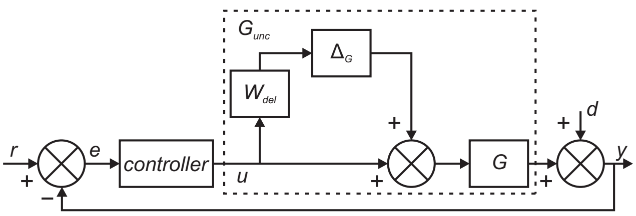

Fig. 8: Uncertain feedback system.

The uncertainty in the input is 10 % in the low frequency range, 100 % at $w = 10^6$ Hz and 1000 % in the high frequency range.

Figure 9 compares the upper bounds of the structured singular values, for the robust stability analysis of the closed-loop systems with the three controllers (1-DOF PID, 2-DOF PID and MS-LS control). To achieve robust stability, it is necessary that the μ-values are less than 1 over the frequency range [28] and [29]. It is clear that the controllers achieve a robust stability. The best robustness is obtained by the MS-LS controller.

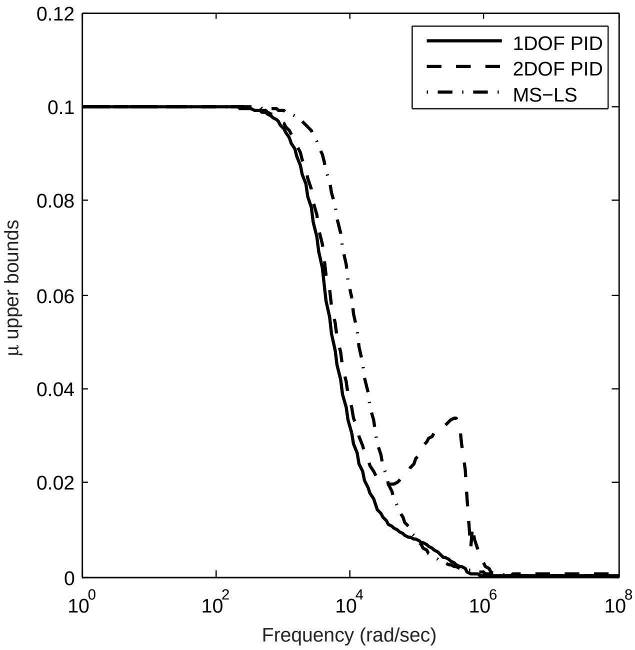

Fig. 9: QBC closed-loop robust stability.

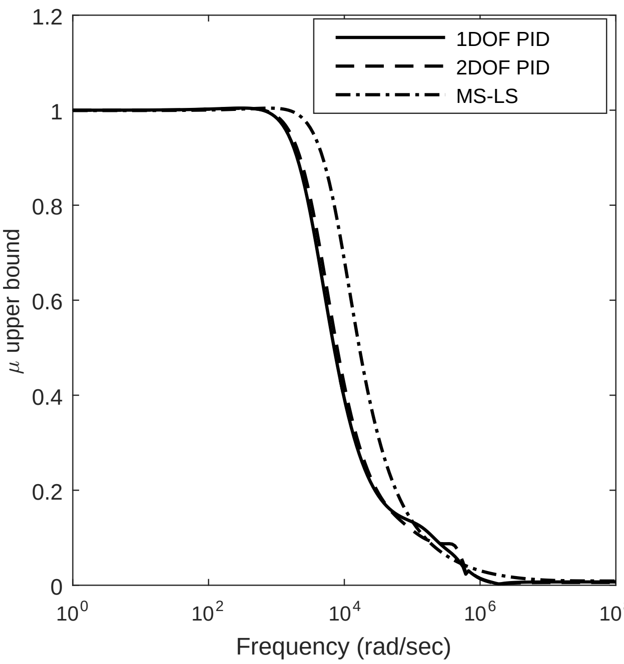

Fig. 10: QBC closed-loop robust performance.

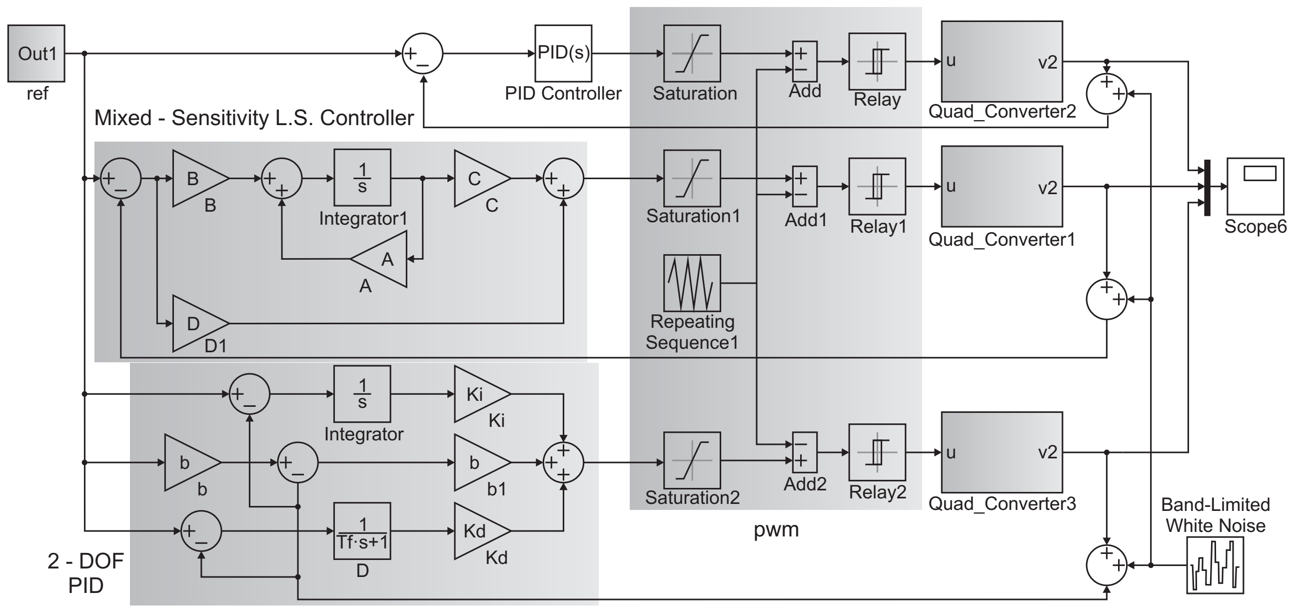

Fig. 11: Simulation block diagram.

The robust performance is achieved if and only if for each frequency computed for the closed-loop frequency response is less than 1. The robust performance tests for the three controllers are shown in Fig. 10. Again, the MS-LS controller shows large μ values over the low-frequency range.

6. Simulation Results

As shown in Fig. 11, the three controllers designed in the above section are implemented in Matlab/Simulink. Note that MS-LS controller $K_r(s)$ is implemented using the state space realization (A, B, C, D). To compare the three controllers' performances and robustness, the following tests are performed.

6.1. Set Point Tracking

The QBC response for a 10 V constant reference voltage is shown in Fig. 12. It can be observed that QBC settling time is 1 ms for the MS-LS control and 2-DOF PID controls, which is faster as compared to the 1.6 ms settling time for the 1-DOF PID control. Another aspect is that MS-LS control exhibits an overshoot of 16.5 %; while the overshoot for the 1-DOF PID and 2-DOF PID is of the order of 15.5 %.

In addition, when the reference input voltage changes from 10 to 12 V, as shown in Fig. 13, an oscillatory behavior is observed for MS-LS control. Comparison to that PID controllers provide a more dumped behavior, in response to the reference voltage increase

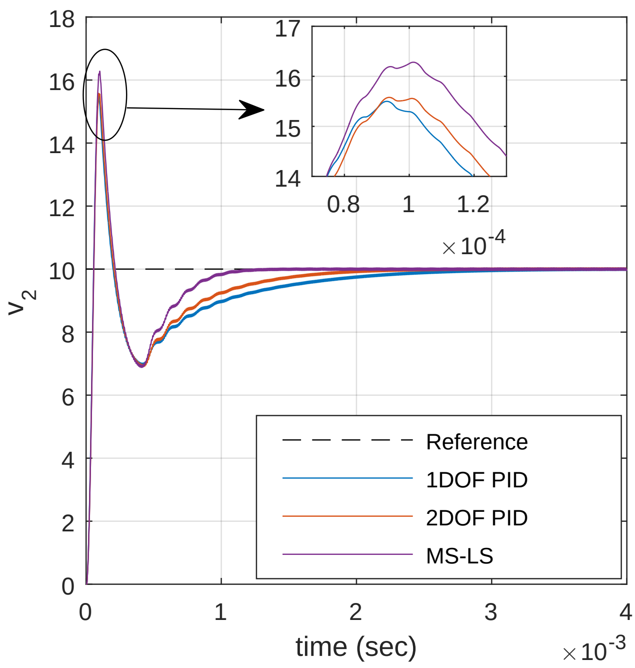

Fig. 12: QBC response to 10 V reference voltage.

or decrease, as can be noticed from Fig. 14 and Fig. 15.

6.2. Load Variation

A load variation of 100 % (from 10 to 20 Ω) is introduced between 10 and 30 ms. QBC response shown in Fig. 16 indicates that all control methods provide almost the same performance. The output voltage exhibits an undershoot of 6 % and an overshoot of 8 %.

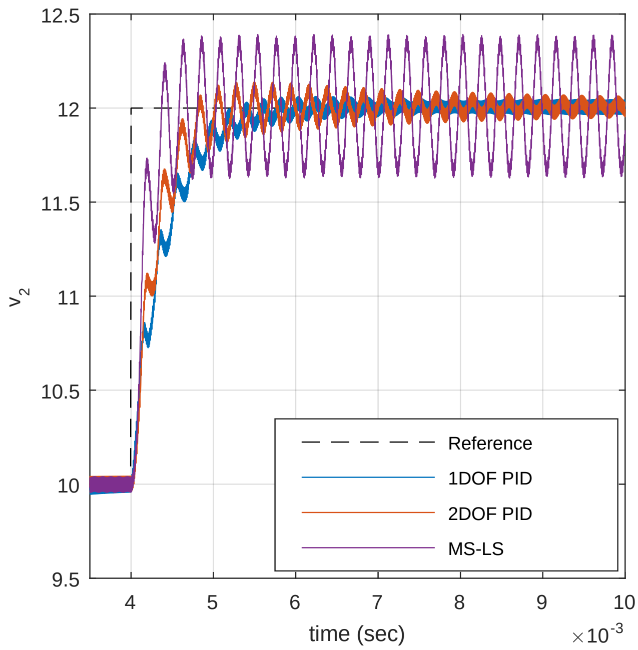

Fig. 13: QBC response to reference voltage change from 10 to 12 V.

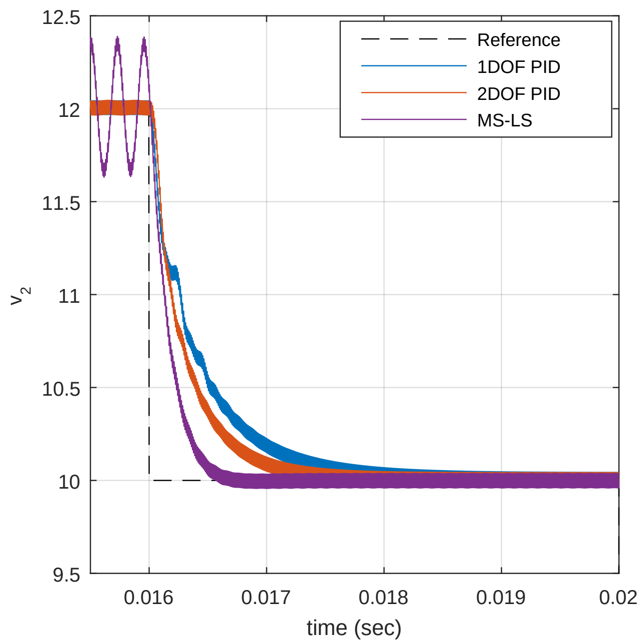

Fig. 14: QBC response to reference voltage change from 12 to 10 V.

6.3. Supply Voltage Variation

A voltage drop of 3 V is introduced in the supply voltage between 5 and 10 ms. Figure 17 shows that the three control methods obtained almost the same stabilizing time with same undershoot (about 7 % at 5 ms). At 10 ms, similar overshoot (35 %) is observed for the three control methods. However, at 10 ms, PID control

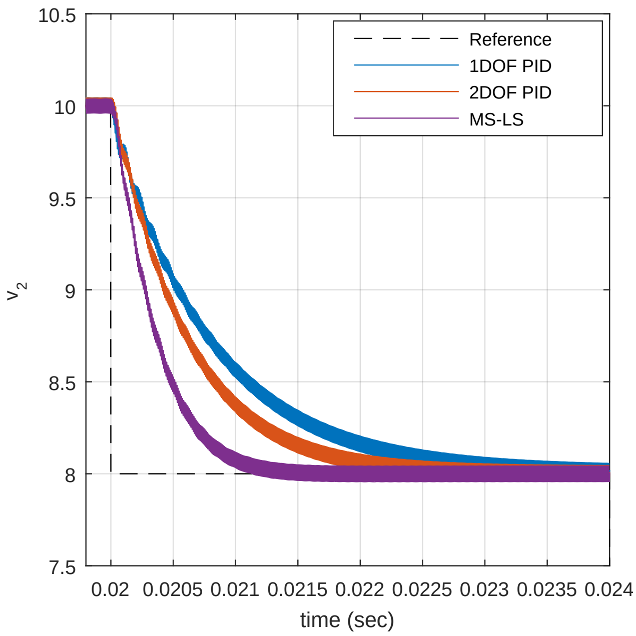

Fig. 15: QBC response to reference voltage change from 10 to 8 V.

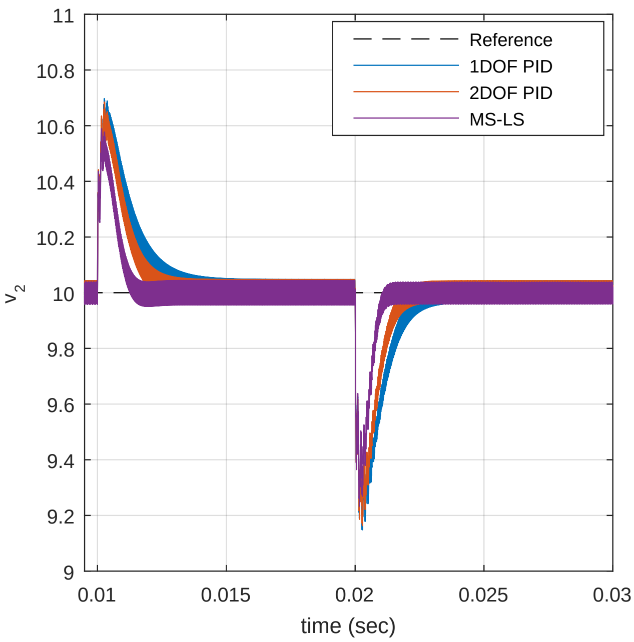

Fig. 16: QBC response to load resistance change.

methods exhibit a null undershoot compared to 3 % for MS-LS control.

6.4. Disturbance Rejection

The supply voltage is perturbed by a sinusoidal component of 100 Hz frequency and 2 V peak-to-peak amplitude. Further, sensor white noise, of 10^8 rad·s^{-1} frequency and 10^{-5} power, is assumed to be superposed on the output voltage. Figure 18 shows that

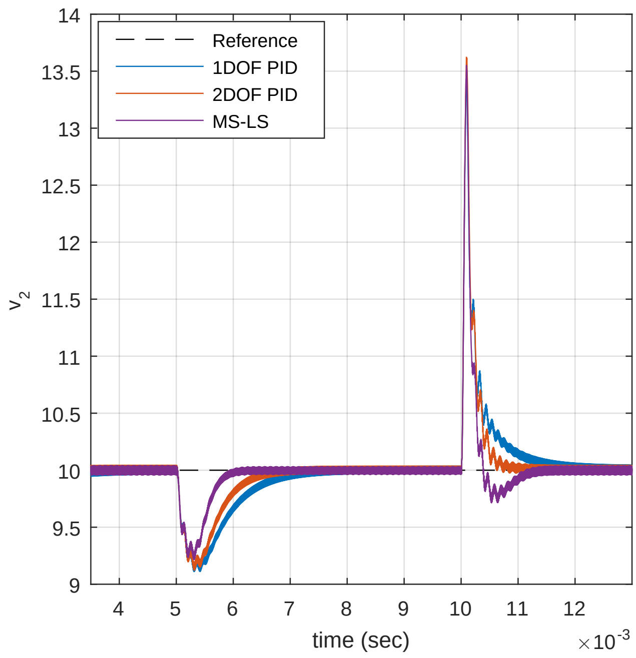

Fig. 17: QBC response to supply voltage change.

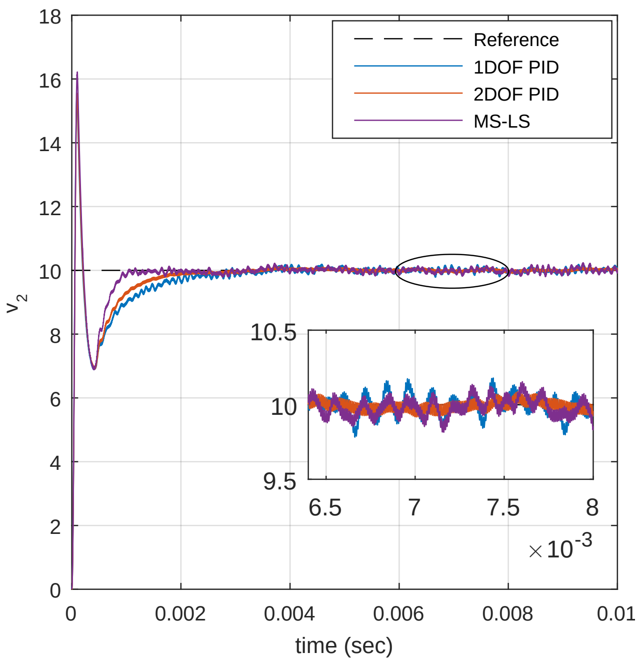

Fig. 18: QBC response to sinusoidal component in power source and white noise.

2-DOF PID controller has better disturbance rejection than 1-DOF PID and MS-LS controllers in this band of frequencies.

7. Conclusion

A 2-DOF PID controller is proposed, designed and simulated for the quadratic buck converter. For comparison purpose, 1-DOF PID and MS-LS control controllers are also tested. Even if MS-LS control shows a faster response, 2-DOF PID provides more duped and accurate response. Further, under perturbations and uncertainties, 2-DOF PID control exhibits better robustness in performance and stability compared to MS-LS control. Another practically important advantage of the 2-DOF PID is a lower structure complexity compared to MS-LS control.

References

[1] BACHA, S., I. MUNTEANU and A. I. BRATCU. *Power electronic converters modeling and control: with case studies*. London: Springer, 2014. ISBN 978-1-4471-5477-8.

[2] TOLLE, T., T. DUERBAUM and R. ELFERICH. Switching loss contributions of synchronous rectifiers in VRM applications. In: *IEEE 34th Annual Power Electronics Specialist Conference 2003*. Piscataway: IEEE, 2003, pp. 144–149. ISBN 0-7803-7754-0. DOI: 10.1109/PESC.2003.1218287.

[3] MATSUO, H. and K. HARADA. The cascade connection of switching regulators. *IEEE Transactions on Industrial Applications*. 1976, vol. IA-12, iss. 2, pp. 192–198. ISSN 0093-9994. DOI: 10.1109/TIA.1976.349401.

[4] MAKSIMOVIC, D. and S. CUK. Switching converters with wide DC conversion range. *IEEE Transactions on Power Electronics*. 1991, vol. 6, iss. 6, pp. 151–157. ISSN 0885-8993. DOI: 10.1109/63.65013.

[5] BARBOSA, L. R., J. B. VIEIRA, L. C. FREITAS, M. S. VILELA and V. J. FARIAS. A buck quadratic PWM soft-switching converter using a single active switch. *IEEE Transactions on Power Electronics*. 1999, vol. 14, iss. 3, pp. 445–453. ISSN 0885-8993. DOI: 10.1109/63.761688.

[6] PACHECO, V. M., A. J. DO NASCIMENTO, V. J. FARIAS, J. B. VIEIRA and L. C. DE FREITAS. A quadratic buck converter with lossless commutation. *IEEE Transactions on Industrial Electronics*. 2000, vol. 47, no. 2, pp. 264–272. ISSN 0278-0046. DOI: 10.1109/41.836341.

[7] REYES-MALANCHE, J. A., N. VAZQUEZ and J. LEYVA-RAMOS. Switched-capacitor quadratic buck converter for wider conversion ratios. *IET Power Electronics*. 2015, vol. 8, iss. 12, pp. 2370–2376. ISSN 1755-4535. DOI: 10.1049/iet-pel.2014.0755.

[8] CARBAJAL-GUTIERREZ, E. E., J. A. MORALES-SALDANA and J. LEYVA-RAMOS. Modeling of a single-switch quadratic buck converter. *IEEE Transactions on Aerospace and Electronic Systems*. 2005, vol. 41, iss. 4, pp. 1450–1456. ISSN 0018-9251. DOI: 10.1109/TAES.2005.1561895.

[9] AYACHIT, A. and M. K. KAZIMIERCZUK. Steady-state analysis of PWM quadratic buck converter in CCM. In: *IEEE 56th International Midwest Symposium on Circuits and Systems (MWSCAS)*. Columbus: IEEE, 2013, pp. 49–52. ISBN 978-1-4799-0065-7. DOI: 10.1109/MWSCAS.2013.6674582.

[10] SIRA-RAMIREZ, H. and R. SILVA-ORTIGOZA. *Control Design Techniques in Power Electronics Devices*. London: Springer-Verlag, 2006. ISBN 978-1-84628-458-8.

[11] WEI, X. L., K. M. TSANG and W. L. CHAN. Non-linear PWM control of single-switch quadratic buck converters using internal model. *IET Power Electronics*. 2009, vol. 2, iss. 5, pp. 475–483. ISSN 1755-4535. DOI: 10.1049/iet-pel.2008.0170.

[12] SOSA, J. M., E. D. SILVA-VERA, G. ESCOBAR, P. R. MARTINEZ-RODRIGUEZ and A. A. VALDEZ-FERNANDEZ. Control design for a quadratic buck converter with LC input filter. In: *IEEE 13th International Conference on Power Electronics (CIEP)*. Guanajuato: IEEE, 2016, pp. 149–154. ISBN 978-1-5090-1775-1. DOI: 10.1109/CIEP.2016.7530747.

[13] ALONGE, F., R. RABBENI, M. PUCCI and G. VITALE. Identification and robust control of a quadratic DC/DC boost converter by Hammerstein model. *IEEE Transactions on Industry Applications*. 2015, vol. 51, iss. 5, pp. 3975–3985. ISSN 0093-9994. DOI: 10.1109/TIA.2015.2416154.

[14] MORALES, J. A. S., J. LEYVA-RAMOS, E. E. G. CARBAJAL and M. G. ORITZ-LOPEZ. Average current-mode control scheme for a quadratic buck converter with a Single switch. *IEEE Transactions on Power Electronics*. 2008, vol. 23, iss. 1, pp. 485–490. ISSN 0885-8993. DOI: 10.1109/TPEL.2007.910907.

[15] BEVRANI, H., P. BABAHAJYANI, F. HABIBI and T. HIYAMA. Robust control design and implementation for a quadratic buck converter. In: *International Power Electronics Conference IPEC-2010*. Sapporo: IEEE, 2010, pp. 99–103. ISBN 978-1-4244-5394-8. DOI: 10.1109/IPEC.2010.5543644.

[16] JIN, Q. B. and Q. LIU. Analytical IMC-PID design in terms of performance/robustness tradeoff for integrating processes: From 2-Dof to 1-Dof. *Journal of Process Control*. 2014, vol. 24, iss. 3, pp. 22–32. ISSN 0959-1524. DOI: 10.1016/j.jprocont.2013.12.011.

[17] MORALES, J. A. S., L. P. RODRIGO and P. H. ELVIA. Parameters selection criteria of proportional-integral controller for a quadratic buck converter. *IET Power Electronics*. 2014, vol. 7, iss. 6, pp. 1527–1535. ISSN 1755-4535. DOI: 10.1049/iet-pel.2013.0343.

[18] XU, G., D. SHA and X. LIAO. Decentralized inverse-droop control for input-series-output-parallel DC-DC converters. *IEEE Transactions on Power Electronics*. 2015, vol. 30, iss. 9, pp. 4621–4625. ISSN 0885-8993. DOI: 10.1109/TPEL.2015.2396898.

[19] APKARIAN, P. and D. NOLL. Nonsmooth H_∞ Synthesis. *IEEE Transactions on Automatic Control*. 2006, vol. 51, iss. 1, pp. 71–86. ISSN 0018-9286. DOI: 10.1109/TAC.2005.860290.

[20] AYACHIT, A. and M. K. KAZIMIERCZUK. Open-loop small-signal transfer functions of the quadratic buck PWM DC-DC converter in CCM. In: *IEEE 40th Annual Conference of the Industrial Electronics Society*. Dallas: IEEE, 2014, pp. 1643–1649. ISBN 978-1-4799-4032-5. DOI: 10.1109/IECON.2014.7048723.

[21] WLODZIMIERZ, J. Small-signal transmittances of DC-DC step-down PWM converter in various operation modes. *Archives of Electrical Engineering*. 2015, vol. 64, iss. 3, pp. 505–529. ISSN 2300-2506. DOI: 10.2478/aee-2015-0038.

[22] STEIGLITZ, K. and L. E. MCBRIDE. A technique for the identification of linear systems. *IEEE Transactions on Automatic Control*. 1965, vol. 10, iss. 4, pp. 461–464. ISSN 0018-9286. DOI: 10.1109/TAC.1965.1098181.

[23] KOLLAR, I., G. FRANKLIN and R. PINTELON. On the equivalence of z-domain and s-domain models in system identification. In: *IEEE Instrumentation and Measurement Technology Conference*. Brussels: IEEE, 1996, pp. 14–19. ISBN 0-7803-3312-8. DOI: 10.1109/IMTC.1996.507191.

[24] ZHOU, K. and J. C. DOYLE. *Essentials of Robust Control*. Upper Saddle River: Prentice-Hall, 1999. ISBN 978-0135258330.

[25] SAFONOV, M. G. and R. Y. CHIANG. A Schur method for balanced-truncation model reduction. *IEEE Transactions on Automatic Control*. 1989,

vol. 34, iss. 7, pp. 729–733. ISSN 0018-9286. DOI: 10.1109/9.29399.

[26] APKARIAN, P. and P. GAHINET. Decentralized and fixed-structure H∞ control in Matlab. In: *50th IEEE Conference on Decision and Control and European Control Conference*. Piscataway: IEEE, 2011, pp. 8205–8210. ISBN 978-1-61284-800-6. DOI: 10.1109/CDC.2011.6160298.

[27] APKARIAN, P., M. N. DAO and D. NOLL. Parametric robust structured control design. *IEEE Transactions on Automatic Control*. 2015, vol. 60, iss. 7, pp. 1857–1869. ISSN 0018-9286. DOI: 10.1109/TAC.2015.2396644.

[28] FAN, M. K. H., A. L. TITS and J. DOYLE. Robustness in the presence of mixed parametric uncertainty and unmodeled dynamics. *IEEE Transactions on Automatic Control*. 1991, vol. 36, iss. 1, pp. 25–38. ISSN 0018-9286. DOI: 10.1109/9.62265.

[29] YEDAVALLI, R. K. *Robust control of uncertain dynamic systems. A linear state space approach*. New York: Springer, 2014. ISBN 978-1-4614-9131-6.

About Authors

Fateh OUNIS was born in Oum El Bouaghi, Algeria. He received the Master degree in electrical engineering from Oum El Bouaghi University, in 2009. Actually, he is finalising Ph.D. thesis. His research interests are power converters design and control.

Noureddine GOLEA received his Doctorate degree in 2001 from Batna University, Algeria. Currently, he is a full Professor in Electrical Engineering Department at Oum El Bouaghi University, Algeria. His research interests are non-linear control, intelligent control and power systems control.

Appendix A Quadratic Buck Converter Parameters

Circuit parametrs	**Values**
Input voltage E	24 V
Reference voltage v_2	10 V
Switching frequency f	110 kHz
L_1	39 µH
L_2	27 µH
C_1	16 µF
C_2	18 µF
$r_{L_1}, r_{L_2}, r_{C_1}, r_{C_2}$	0.25 Ω
Load R	10 Ω